Investigation of the effects of high cervical spinal cord electrical stimulation on improving neurological dysfunction and its potential mechanism in rats with traumatic brain injury

Peng-Cheng Zhao[a,b], Zhen-Shan Huang[a], Shao-Nian Xu[a], Peng-Cheng Deng[a], Feng Qian[a], Jian Shi[a] and Yong-Ming Zhang[a]

To explore the effects of high cervical spinal cord electrical stimulation (cSCS) on the recovery of neurological function and its possible mechanism in rats with traumatic brain injury (TBI). 72 rats were randomly divided into: (1) a sham group; (2) a traumatic brain injury (TBI) group; (3) a TBI+cSCS group; (4) a LY294002+TBI+cSCS group. The degree of neurological dysfunction was evaluated by modified Neurological severity score (mNSS). The pathological changes of the brain tissue in the injured area were observed by HE staining, and the apoptosis of neuron cells were observed by TUNEL staining. The expressions of BDNF and VEGFmRNA were detected by polymerase chain reaction (PCR), and the expressions of p-AKT, AKT, Bcl-2, Bax and caspase-3 proteins were detected by western blot. Compared with that of the TBI and LY294002+TBI+cSCS groups, the mNSS of the TBI+cSCS group were significantly lower on day 3 and 7 ($P < 0.05$). Compared with that in the TBI and LY294002+TBI+cSCS groups, the apoptosis of neuron cells in the TBI+cSCS group decreased significantly ($P < 0.05$). Compared with the TBI and LY294002+TBI+cSCS group, the expression of Bcl-2 protein increased and the expressions of Bax and Caspase-3 proteins decreased in the TBI+cSCS group ($P < 0.05$). Compared with that in the TBI and LY294002+TBI+cSCS groups, the intensity of p-Akt/Akt in the TBI+cSCS group increased ($P < 0.05$). We found that cSCS had a protective effect on neuron cells after craniocerebral injury and could improve neurological dysfunction in rats, the mechanism of which might be that cSCS made the PI3K/Akt pathway more active after TBI. *NeuroReport* 33: 509–517 Copyright © 2022 The Author(s). Published by Wolters Kluwer Health, Inc.

Introduction

Traumatic brain injury (TBI) is generally regarded as a type of brain damage caused by external factors, which is one of the main causes of disability and death in patients of all ages, and is a major challenge to public health worldwide [1]. To date, the 'landmark' events of consciousness disorder caused by delayed secondary central nervous system injury include the Wallerian degeneration of axons, mitochondrial dysfunction, excitotoxicity, oxidative stress, apoptosis, and the cell death of neurons and glial cells [2]. A series of changes in intracranial neurochemistry, metabolism, cells, and molecules often lead to a decrease in consciousness level and cognitive impairment [3]. To date, extensive research has been devoted to identifying treatable targets related to these processes.

Spinal cord electrical stimulation (SCS) is primarily used by placing a stimulation electrode within the epidural space of the corresponding spinal cord segment via surgery; then, using pulse-width transmission modes, specific frequencies and amplitudes, and by regulating the electric signal transmission in autonomic, peripheral, and central nerves, the purpose of this treatment can be achieved [4]. Existing studies have shown that SCS can prevent cell apoptosis in rats with Parkinson's disease (PD) and promote brain plasticity and functional recovery in rats with cerebral ischemia [5,6]. In addition, Xu *et al.* [7] reported on a clinical trial involving 12 patients with cognitive impairment who underwent SCS and were followed up for an average of 11 months. Subsequently, five patients achieved responsive results and seven showed

no response. The authors proposed cervical SCS (cSCS) as a suggested treatment for patients with cognitive impairment. Few studies, however, have been conducted on whether SCS can reduce neuroinflammation and apoptosis following TBI and improve cognitive function in rats. Accordingly, the current study aimed to explore the role and potential mechanism of SCS in neuroinflammation and apoptosis after TBI using a rat model.

Materials and methods

This study was conducted in accordance with the declaration of Helsinki. This study was conducted with approval from the Ethics Committee of Anhui Medical University, China.

Animals

Compared to the male rats, female rats usually have much more obvious hormonal changes due to the estrous and menstrual cycles. In order to avoid the interference from the hormonal changes, the male rats were used in this present study. A total of 72 clean-grade Sprague–Dawley male rats with a body weight of 200 ± 20 g were purchased from Jinan Pengyue Experimental Animal Breeding Co., Ltd. (Jinan City, Shandong Province China) and raised in the experimental animal center of Anhui Medical University under the same living conditions concerning factors such as temperature, humidity, 12 h light/dark cycles, and providing the correct amount of water and professional rat feed. After 7-day feeding, the rats were used to carry out our experiment. A completely randomized design was performed, and the details were as follows: the Excel was used; the animal numbers in ascending order in the first column were arranged; random numbers were generated in the second column using the 'RAND ()' function; the two columns were copied, and pasted in the new sheet by 'value'; the column of the random numbers were arranged in ascending order together with the animal numbers; finally according to the row number, beginning from the first row, every continuous 18 rows were selected as one group in sequence. Finally, all rats were randomly divided into the following four groups: (1) a sham group; (2) a TBI group; (3) a TBI + cSCS group; (4) a LY294002 (PI3K inhibitors) + TBI + cSCS group, with 18 rats in each group. All rats in each group were evaluated by a neurological dysfunction score on days 3 and 7 after cSCS. Four rats in each group were used for hematoxylin-eosin (HE) staining on days 7 after cSCS. Four rats in each group were used for terminal deoxynucleotidyl transferase-mediated dUTP nick end labeling (TUNEL) staining on days 7 after cSCS. Five rats in each group were used for fluorescence quantitative fluorescence PCR on days 7 after cSCS. Five rats in each group were used for western blot analysis on days 7 after cSCS.

Reagents

Hematoxylin staining solution (ZLI-9610; ZSGB-BIO, Beijing City, China); Eosin staining solution (G1100; Solarbio, Beijing City, China); Scott TapWater/Bluing (G1865; Solarbio); TUNEL assay kit (C1088; Beyotime, Shanghai City, China); Super ECL plus (RJ239676; Thermo Fisher, Shanghai City, China); Trizon Reagent (CW0580S; CWBIO, Beijing City, China); Ultrapure RNA Extraction Kit (CW0581M; CWBIO); HiScript II Q RT SuperMix for qPCR (+gDNA wiper) (R223-01; Vazyme, Nanjing City, Jiangsu, China); 2 × SYBR Green PCR Master Mix (A4004M; Lifeint, Xiamen City, Fujian Province, China); RIPA Lysis Buffer (C1053; PPLYGEN, Beijing City, China); BCA Protein Assay Kit (CW0014S; CWBIO); 1M Tris-HCL buffer (PH = 6.8) (T1020; Solarbio); 1.5M Tris-HCL buffer (PH = 8.8) (T1010; Solarbio); SDS (151-21-3; Xilong Scientific, Shantou City, Guangdong Province, China); TEMED (T105496; Aladdin, Shanghai City, China); Marker (#26617; Thermo Fisher); PVDF (IPVH00010; Millipore, Shanghai City, China); skimmed milk powder (P1622; PPLYGEN); Internal reference primary antibody: Mouse Monoclonal Anti-GAPDH (TA-08, ZSGB-BIO, 1/2000); Secondary antibody: HRP-conjugated Goat anti-Mouse IgG (H+L) (ZB-2305, ZSGB-BIO, 1/2000); Akt rabbit antibody (10176-1-AP; Proteintech, 1/500, Shanghai City, China); p-AKT rabbit antibody (af0832; Affinity, 1/500, Shanghai City, China); Bax rabbit antibody (50599-2-lg; Proteintech, 1/500, Beijing City, China); Bcl-2 rabbit antibody (bs-34012R; Bioss, 1/500, Shanghai City, China); caspase-3 rabbit antibody (af6311; Affinify, 1/500, Shanghai City, China); BSA (A8020; Solarbio).

Traumatic brain injury model

ZH-ZYQ free fall brain injury model striker was purchased from Anhui zhenghua biologic apparatus facilities co., ltd to induce TBI model. Except for the sham group, based on conventional methods, the TBI models [8] were established within the remaining groups. The rats were anesthetized via intraperitoneal injection of 1% sodium pentobarbital (80 mg/kg). The skin at the top of the skull was prepared and disinfected; then, the skull was fixed using astereotactic instrument. Subsequently, we made a midline scalp incision to fully expose the skull and drilled a circular bone hole of 5 mm in diameter with the edges 5 mm posterior to the coronal suture and 5 mm on the right side of the sagittal suture. Next, we performed the cortical impact at the bone hole using a 25 g weight by vertically dropping it from a height of 25 cm. For the rats in the sham group, we only drilled bone holes without cortical impact. Following surgery, the rats were placed in cages equipped with heating pads until they recovered from anesthesia.

The cervical spinal cord electrical stimulation model

Using layer-by-layer separation along the midline of the spine at the C1–C4 level, the lamina, dura mater, and intervertebral space were exposed. The C2 spinous process of the rat was slowly lifted with tweezers to open the field of vision to the intervertebral space. This process

should be performed with care to avoid damaging the rat's spinal cord. Next, the head-end of the stimulating electrode enamel wire was bent into an L-shape and slowly implanted without puncturing the dura mater. Next, the tail-end of the enameled wire was closely sutured and fixed with dental bone cement, and the subcutaneous tunnel was penetrated from the back to ensure that the stimulation wire was always located in the intervertebral space during the rat's daily activities. Following stimulation, it was found that the neck muscles vibrated slightly, indicating that modeling of the cSCS had been successful. One day after establishing the TBI model, the cSCS and inhibitor rat groups were given electrical stimulation using aBL420 electrical stimulator; unipolar stimulation was used at a frequency of 50 Hz, a pulse width of 100 µs, and a current of 0.4–0.6 mA [9]. SCS was performed every 10 min for 2 min for a total of 30 min once a day over seven consecutive days [10].

Lateral ventricle injection
In the model inhibitor group, 10 µl LY294002 (PI3K inhibitor) was injected into the lateral ventricle for 0.5 h before affecting the craniocerebral injury. After administering anesthesia, the rats were fixed on a brain stereotactic instrument. The size of the bone window was located according to the specific injection site (0.8 mm behind the anterior fontanelle, 1.5 mm outside the midline, and 3.5 mm deep). Then, the skull was exposed. After opening the hole with a hand-held drill, LY294002 was injected at 1 µl per minute [11]. During injection, attention was focused on retaining the needle perpendicular to the skull plane.

Neurological dysfunction score
On days 3 and 7 after cSCS, the degree of neurological deficit was evaluated using a modified neurological severity score (mNSS) [12] which included motor, sensory, reflex, and balance tests. Scores were analyzed by observers blinded to the experimental cohort. The score ranged from 0 to 18 according to the severity of injury. The higher score indicated the most severe injury (0, no injury; 1–6, mild injury; 7–12, average moderate injury; 13–18, severe injury; 18, maximum injury). The details of the mNSS were shown in supplementary table 1, Supplemental digital content 1, *http://links.lww.com/WNR/A661*.

Brain tissue preparation
After anesthetizing the rat, a large amount of iced saline was perfused into the left ventricle, and after the liver turned white, a small amount of 4% polyformaldehyde was perfused. After the whole body of the mouse was stiffened, the head was cut off and the whole brain tissue was taken out and placed on the operating table. The brain tissue around the brain injury was used as a research sample. This process was completed at a constant temperature of 4 °C.

Hematoxylin-eosin staining
Brain tissue sections (five sections per sample) were collected for fixation, dehydration, and transparent rendering in ethanol and xylene solutions. The sections were then embedded in wax. The paraffin sections were baked and dewaxed and placed in a hematoxylin solution after hydration for 3 min. Next, the sections were washed with pure water; hydrochloric acid ethanol in a differentiation solution was then added for 15 s and the sections were again washed with pure water. Next, a diluted ammonia blue solution was added to the sections for 15 s before they were again washed with pure water. Then, the eosin solution was applied to the sections for 3 min before they were fully washed three times (5 min each) using PBS. After sealing the sections, cell and tissue morphologies were observed using a microscope. The nucleus was blue-purple and the cytoplasm was red.

Terminal deoxynucleotidyl transferase-mediated dUTP nick-end labeling staining
The brain tissue sections (five sections per sample) were dewaxed twice for 10 min each time using xylene solution, then were soaked in a gradient ethanol solution (100, 95, 90, 80, 70%) in sequence, 5 min each time, and finally were washed by PBS twice. Followingly, the sections were treated with 50 µg/ml Proteinase K solution at 37 °C for 30 min. The sections were washed three times with PBS (5 min each time). The prepared TUNEL staining solution was added to each section, and they were incubated at 45 °C for 2 h. After quenching the seal with anti-fluorescence, the sections were observed under a fluorescence microscope. The nucleus of cells was fluorescent blue, and the apoptotic cells were fluorescent green. Data were expressed as the ratio of apoptotic cells to total cells.

Real-time fluorescence quantitative PCR
The primers were designed and synthesized by General Biosystems (Anhui) Co., Ltd. (see Table 1 for primer sequences). β-actin was used as the internal reference gene. The PCR was conducted according to the $2 \times$ SYBR Green PCR Master Mix instructions. LightCycler480 cycle conditions: 10 min Taq hotstart activation at 95 °C was performed, followed by 40 cycles of denaturation at 95 °C for 15 s, annealing at 60 °C for 30 s, and extension at 72 °C for 30 s. The final step comprised cooling to 50 °C for 30 seconds. After the average value was obtained, cycle threshold value was calculated by $2^{-\Delta\Delta Ct}$ Method.

Western blot
Western blotting was conducted to detect the expression levels of protein kinase B (p-AKT), protein kinase B (AKT), B-cell lymphoma-2 (Bcl-2), Bax, and caspase-3 proteins in brain tissue following brain contusion. A sample of contused brain tissue (~100 mg) was ground in a homogenizer, and primary antibodies p-AKT, AKT

Table 1 Primer sequence

Primer name	Primer sequence	Primer length (nt)	Product length (bp)	Annealing temperature (°C)
VEGF F	AATTGAGACCCTGGTGGACA	20	246	58.5
VEGF R	CTATCTTTCTTTGGTCTGCATTCAC	25		
BDNF F	AGCCTCCTCTGCTCTTTCTG	20	258	58.9
BDNF R	TGGGATTACACTTGGTCTCGT	21		
β-actin F	GCCATGTACGTAGCCATCCA	20	375	59.5
β-actin R	GAACCGCTCATTGCCGATAG	20		

BDNF, brain-derived neurotrophic factor.

(1:1000; Abcam, Shanghai City, China), Bcl-2, Bax, and caspase-3 (1:500; Proteintech) were added, incubated overnight at 4 °C, and washed on a tris buffered saline with Tween membrane (10 min, ×3). After washing, it was incubated with the corresponding secondary antibody (1:1000) for 2 h at room temperature, and an electrochemiluminescent agent was added to achieve a color reaction. The ratio of the gray value of the target protein band to the gray value of the glyceraldehyde 3-phosphate dehydrogenase band reflected the expression level of the target protein.

Statistical analysis
All data were statistically analyzed using the SPSS Statistics 19.0 software program. One-way ANOVA followed by Bonferroni's multiple comparison post-hoc test was performed. The data were expressed as mean ± SD (x ± SD), and $P < 0.05$ was considered statistically significant.

Results
Comparison of modified neurological severity score of rats between groups
As shown in Fig. 1, compared with that of the sham group, the mNSS of the TBI group significantly increased on days 3 and 7 ($P < 0.001$); compared with that of the TBI group, the mNSS of the TBI + cSCS group were significantly lower on days 3 ($P < 0.01$) and 7 ($P < 0.001$); compared with that of the LY294002 + TBI + cSCS group, the mNSS of the TBI + cSCS group were also significantly lower on days 3 ($P < 0.05$) and 7 ($P < 0.05$).

Hematoxylin-eosin staining analysis
Under a light microscope, the brain tissue taken from the sham group showed normal physiological characteristics and a large number of normal neurons. In the TBI group, the brain tissue structure was seriously damaged, a large number of inflammatory cells had infiltrated, and hyperemia and hemorrhage were obvious; neuronal swelling, pale staining of the cytoplasm, vacuolization of cell nuclei, the shrinking of some nucleosomes, and neuronal necrosis were observed. For the TBI + cSCS group, the above pathological phenomena had been improved, the congestion and bleeding foci were reduced, the number of inflammatory cells was reduced, the degree of brain tissue damage was low, and the number of neuronal cells increased. Compared with the TBI + cSCS group, the

LY294002 + TBI + cSCS group reflected more severe results, with obvious hyperemia and bleeding, as well as increased neuronal necrosis (Fig. 2).

TUNEL staining analysis
As shown in Fig. 3, compared with that in the sham group, the apoptosis of neuron cells in the TBI group significantly increased ($P < 0.001$); compared with that in the TBI group and the LY294002 + TBI + cSCS group, the apoptosis of neuron cells in the TBI+cSCS group decreased significantly after the administration of cSCS ($P < 0.001$).

The expression of brain-derived neurotrophic factor and vascular endothelial growth factor messenger RNA in the injured brain tissue detected by the reverse transcription-PCR
As shown in Fig. 4, compared with that in the sham group, the expression of brain-derived neurotrophic factor (BDNF) ($P < 0.01$) and vascular endothelial growth factor (VEGF) ($P < 0.001$) messenger RNA (mRNA) in the TBI group increased significantly; compared with that in the TBI group, the expression of BDNF ($P < 0.01$) and VEGF ($P < 0.001$) mRNA in the TBI+cSCS group increased significantly; compared with the LY294002 + TBI + cSCS group, the expression of VEGF mRNA in the TBI + cSCS group increased significantly ($P < 0.05$), while the expression of BNDF mRNA in the TBI + cSCS group did not increase significantly.

The expression levels of Akt, p-Akt, Bax, Bcl-2, and caspase-3 proteins detected by western blots
As shown in Fig. 5, compared with that in the sham group, the expression level of Bcl-2 protein in the TBI group decreased significantly ($P < 0.001$), while the expression levels of Bax and caspase-3 proteins increased significantly ($P < 0.001$); compared with that in the TBI group and LY294002 + TBI + cSCS group, the expression level of Bcl-2 protein in the TBI + cSCS group increased significantly ($P < 0.001$), while the expression levels of Bax and caspase-3 proteins decreased significantly ($P < 0.01$). In addition, compared with that in the sham group, the intensity of p-Akt/Akt in the TBI group decreased significantly ($P < 0.001$). Compared with that in the TBI group and LY294002 + TBI + cSCS group, the intensity of p-Akt/Akt in the TBI + cSCS group increased significantly ($P < 0.001$).

Fig. 1
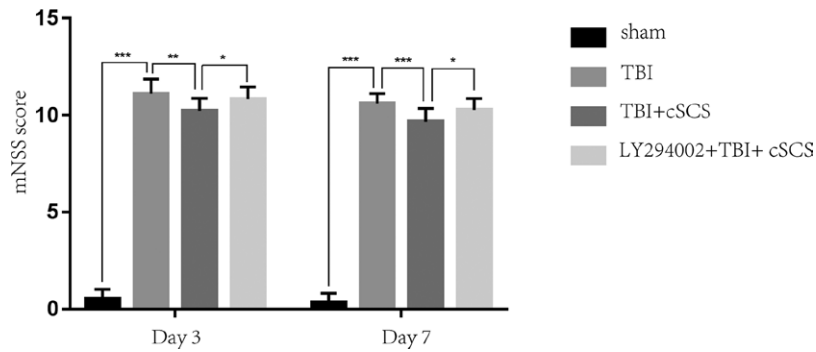
The quantification of modified neurological severity score (mNSS) (x ± SD) on days 3 and 7. ***$P < 0.001$, **$P < 0.01$, and *$P < 0.05$.

Fig. 2
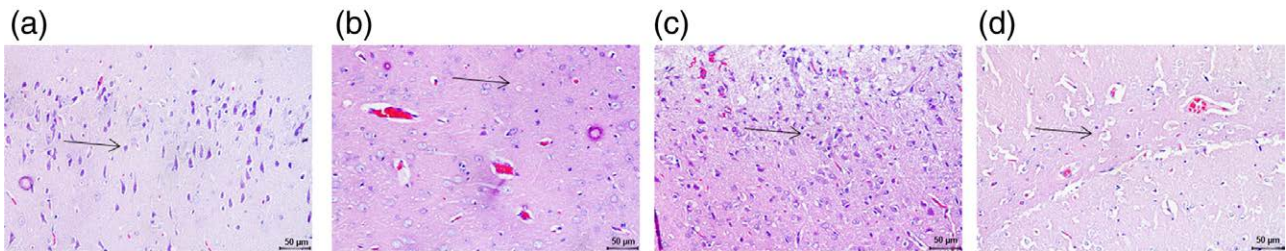
HE staining analysis showed that the brain tissue structure in the TBI group was seriously damaged. Sham group (a); TBI group (b); TBI + cSCS group (c); LY294002 + TBI + cSCS group (d). cSCS, cervical spinal cord electrical stimulation; HE, hematoxylin-eosin; TBI, traumatic brain injury.

Discussion

The pathological manifestations of TBI are characterized by changes in the blood-brain barrier caused by cerebral ischemia, inflammation and a redox imbalance. Early trauma is characterized by the destruction of the blood-brain barrier, a reduction in blood flow, and damage to the neurons and glial cells in the brain. Secondary injury evolves from the primary injury and typically occurs a few hours, days, or months later and may involve several factors, for example, oxidative stress, the regulation of calcium homeostasis, inflammation, and axon injury, which will eventually lead to apoptosis, neural circuit disorders, and impairment in synaptic transmission and plasticity [13]. In terms of behavior, these changes can manifest as posttraumatic headache, depression, personality changes, anxiety, aggression, and attention defects in cognition, sensory processing, and communication. Most moderate and severe TBI can cause acute cell death, which can, in turn, cause secondary injuries such as microglial activation, oxidative stress, inflammation, and autophagy, giving rise to cognitive and behavioral disorders [14].

The social and economic problems related to posttraumatic dysfunction place a heavy burden on medical systems and broader society. A deepening understanding of the clinical characteristics and complex pathophysiological mechanisms of TBI has promoted the development of new and promising treatment methods [15]. As an induced coma and re-awakening approach, the mechanism of SCS in the treatment of cognitive dysfunction after brain injury is still being explored. Only a few basic experiments have been conducted involving the application of SCS to disturbance of consciousness. In terms of cerebral hemodynamics, Broseta *et al.* [16] first increased the carotid and cerebral blood flow of goats, dogs, and rabbits through C1–C2 spinal cord stimulation, and achieved a beneficial vasomotor effect in a rat vasospasm model. Subsequently, studies have shown that cervical SCS causes cerebral vasodilation, which may be related to the indirect effect on changes in the brainstem vascular motor center and sympathetic nerve tension [17]. Recent studies focused on the molecular pathways involved in the regulation of brain and peripheral circulation in SCS animal models. Wu *et al.* [18] demonstrated that SCS activated the transient receptor potential vanillic acid type 1, which includes sensory fibers and produces the release of calcitonin gene-related peptide, which is considered a powerful mediator of vasodilation. Concurrently, data suggest that extracellular regulated protein kinase (ERK) and

Fig. 3
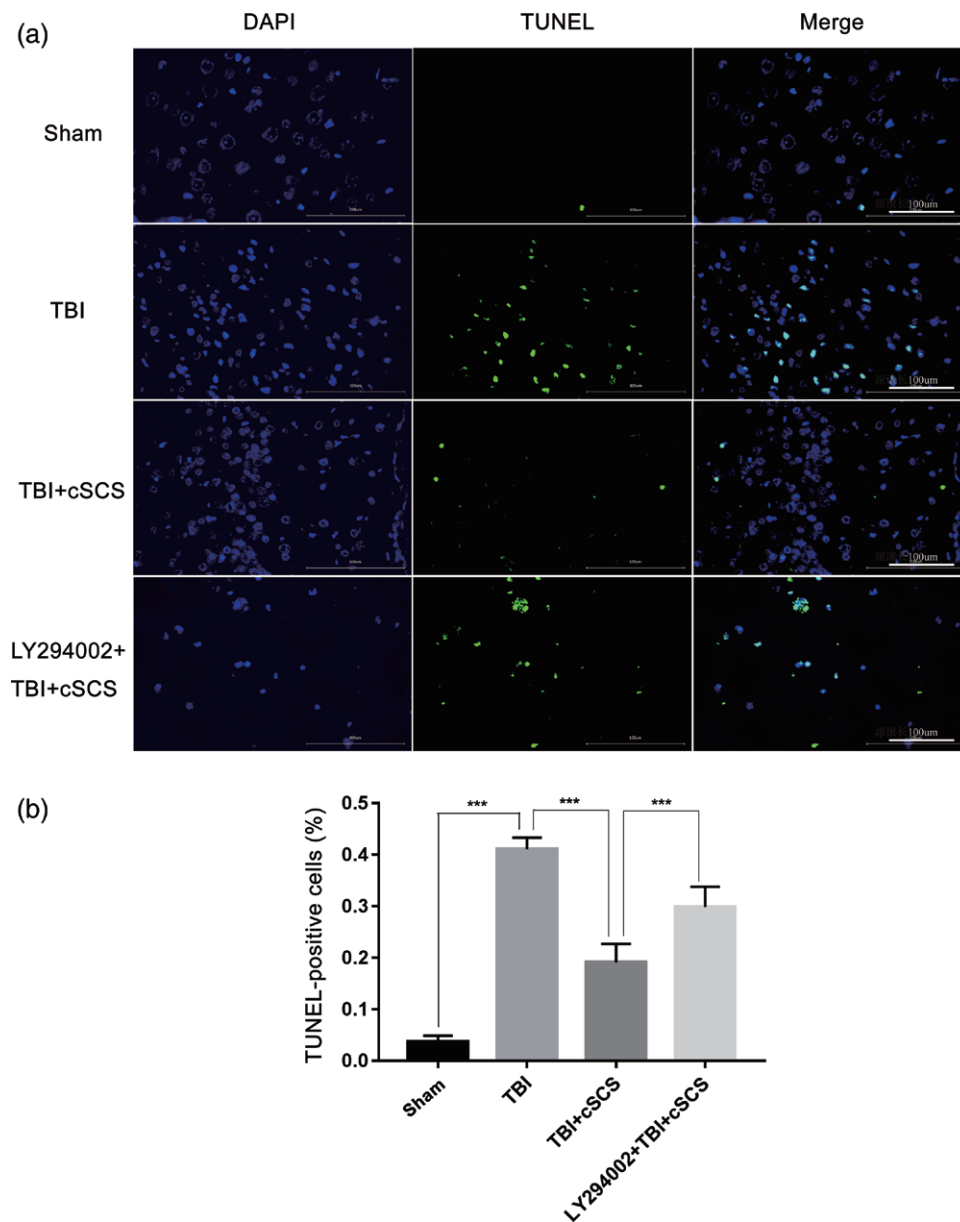
cSCS significantly reduced neuron cells apoptosis caused by TBI. TUNEL was used to detect the cell apoptosis (a and b). ***$P < 0.001$. cSCS, cervical spinal cord electrical stimulation; TBI, traumatic brain injury; TUNEL, transferase-mediated dUTP nick end labeling.

Akt pathways are involved in SCS-induced vasodilation, and also increase neuronal excitability and brain plasticity in rats with cerebral ischemia [6,19]. A recent study aimed to detect Akt/p-Akt, the signal transducer and activator of transcription 3 (STAT3)/p-STAT3, and glycogen synthase kinase (GSK-3) β/p-GSK-3 βin the tissue of white rabbits with spinal cord ischemia-reperfusion (I/R) injury using SCS. The results showed that SCS had a neuroprotective effect on rabbits with spinal cord I/R injuries; its mechanism was indicated as

being related to Akt activation but not related to the independent regulation of STAT3 and GSK-3 β phosphorylation [20].

In our present study, four groups were established, and mNSS was applied to evaluate the degree of neurological dysfunction. Our results showed that the neurological function of rats with TBI was observably impaired. The neurological dysfunction of the TBI + cSCS group was improved significantly, indicating that cSCS might improve spatial memory by significantly reversing the

Fig. 4
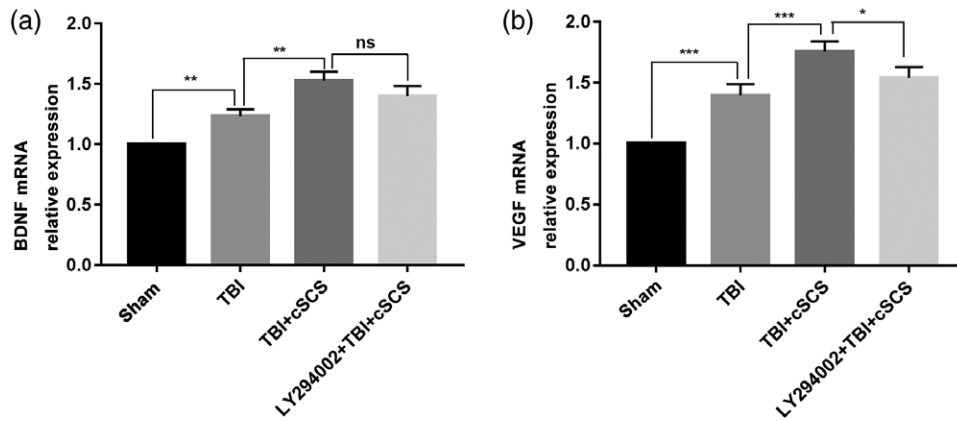
FQ-PCR was used to detect the BDNF mRNA relative expression (a) and VEGF mRNA relative expression (b). ***$P < 0.001$, **$P < 0.01$, *$P < 0.05$. BDNF, brain-derived neurotrophic factor; FQ-PCR, fluorescence PCR; ns, no significance; mRNA, messenger RNA; VEGF, vascular endothelial growth factor.

Fig. 5
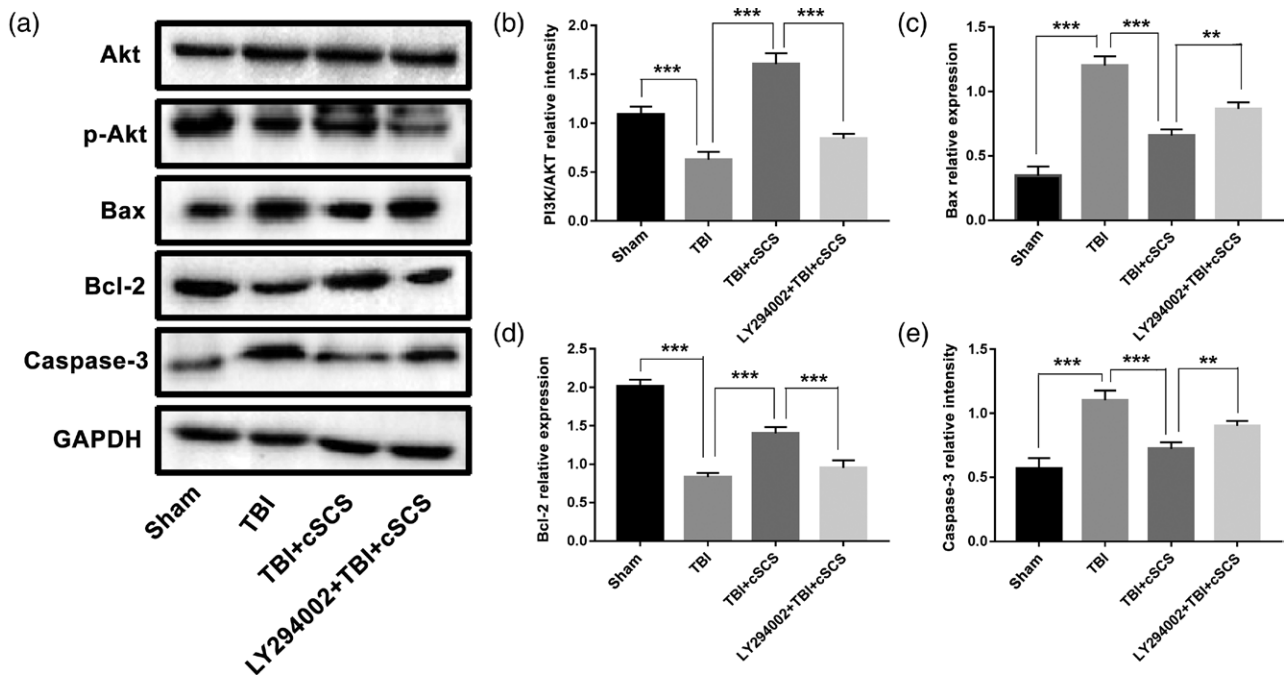
Western blot was used to detect the protein expression levels of Akt, p-Akt, Bax, Bcl-2, and Caspase-3 in brain tissue of the injured area in each group (a). Comparison of PI3K/AKT relative intensity (b), Bax relative expression (c) Bcl-2 relative expression (d), and Caspase-3 relative intensity (e) among groups. ***$P < 0.001$, and **$P < 0.01$.

brain injury caused by trauma and this effect is affected by PI3K receptor blockers.

The results of pathological hematoxylin and eosin staining showed that cSCS improved the pathological structure of brain tissue in rats with a brain injury. Nucleosome pyknosis and neuronal necrosis were significantly less in the stimulated rat group compared with rats in the brain injury group. Furthermore, TUNEL staining showed that the apoptosis of neuron cells in the brain tissue of the injured area increased significantly in the TBI group; moreover, the apoptosis of neuron cells in the brain tissue of the injured area decreased significantly following the application of cSCS, indicating that this procedure could

reduce the apoptosis density of neuron cells in brain-injured rats. The above two phenomena were affected by PI3K receptor blockers.

Apoptosis plays an important role in neuronal loss following craniocerebral injury, which can last for several days and is associated with a poor prognosis [21]. Important programmed death processes include cell-cycle activation-dependent cell death, caspase-mediated apoptosis, the apoptosis of pro-apoptotic members of the Bcl-2 family, poly-ADP ribose polymerase/apoptosis-inducing factor-dependent death, and calpain/tissue-dependent death [22]. In addition, the PI3K/Akt signaling pathway is an important endogenous pathway for regulating cell apoptosis/survival and plays an important role regarding changes in neural function after craniocerebral injury. The PI3K pathway can be activated by several factors to phosphorylate Akt, while activated Akt can inhibit the expression of a series of apoptosis-related genes including caspase-3 [23].

Caspase-3 is an important effector of the caspase family and plays a significant role in neuronal loss after brain injury [24]. The changes in cell morphology following a brain injury, such as nuclear fragmentation and staining condensation, occur through the cleavage of caspase-dependent specific apoptotic substrates. Many studies have reported the relationship between caspase activation and neuronal apoptosis in brain injury. The level of caspase-3 in the cerebrospinal fluid and brain tissue of patients with a brain injury was higher than in a control group [25]. In addition, the level of caspase-3 in dead brain tissue (the ischemic area of a traumatic brain contusion) was also higher than in surviving patients with brain trauma [26]. Bcl-2 and Bcl xL are anti-apoptotic proteins that directly inhibit mitochondrial outer membrane permeabilization (MOMP) or inhibit pro-apoptotic proteins and regulate MOMP and caspases. The increase of their expression assists in supporting cell survival, while the upregulation of Bax, Bad, or BIM promotes cell death after brain injury. The balance between these proteins is the primary determinant of cell death following brain injury [27].

The results of the current study showed that after TBI, the expression levels of Bax and caspase-3 increased, and the expression levels of p-Akt/Akt and Bcl-2 protein decreased. After the administration of cSCS, the expression levels of Bax and caspase-3 decreased, and the expression levels of p-Akt/Akt and Bcl-2 protein increased. These processes can be partially inhibited by PI3K pathway inhibitors. Therefore, we speculate that cSCS can regulate apoptosis after TBI and is related to the PI3K/Akt pathway.

Brain-derived neurotrophic factor is secreted by brain cells and abundant in the brain. It is involved in regulating the growth and survival of existing neurons, as well as the growth and differentiation of new neurons and synapses. In addition, BDNF plays an active role in learning, memory, and sensory-motor recovery by promoting the plasticity of synapses and axons [28]. The PI3K/Akt signaling pathway is closely related to BDNF. Data indicates that PI3K in glial cells may change the expression and secretion of BDNF, and subsequently affect the synaptic transmission between neurons, thereby affecting synaptic plasticity [29]. To investigate the expression of key genes regulated by SCS, microelectrodes were implanted at the L1 vertebral body level in rats with neuropathic pain. Mechanical pain sensitivity tests were carried out after continuous application of SCS for 72 h [30]. The results showed that the continuous application of SCS could regulate neuronal membrane potential and regulate the expression of key genes including BDNF [30].

Vascular endothelial growth factor is a homodimeric growth factor that is structurally expressed in the brain. It is up-regulated during hypoxia and ischemia and is part of the adaptive response to protect tissue from injury [31]. In-vivo studies have shown that, after stroke, when VEGF is locally supplied by the lateral ventricle, it reduces the infarct scope, improves neurological deficits, and prevents delayed neuronal injury by inhibiting caspase-3 [32]. The PI3K/Akt and ERK pathways are two key signaling pathways involved in the protective effect mediated by VEGF activation, which helps to alleviate MPP$^+$-induced neurotoxicity by activating the PI3K/Akt signaling pathway, and confirms that the neuroprotection and angiogenesis of VEGF depend on PI3K/Akt [32].

It has been reported that electrical stimulation has a neuroprotective effect on central nervous system diseases such as cerebral ischemia, brain injury, epilepsy and PD, which may be partly related to VEGF. In a study on SCS, Choi and Lee [6] found that the level of VEGF in the ischemic marginal area was significantly increased, and the level of phosphorylated Akt tended to increase in an SCS group. Another study observed the neuroprotective effect of high cervical SCS treatment on PD model rats, where rats received high cervical SCS (C1–C2) for up to 1 h every day for 16 d. SCS up-regulated the level of VEGF 1 week after injury, suggesting that high SCS in the cervical segment had a neuroprotective effect on PD model rats, at least partially, by up-regulating the expression of VEGF [33].

Based on the above results, our present study demonstrated that cSCS could promote the recovery of neurological functions, which might be partly caused by increasing the levels of VEGF and BDNF in the brain tissue around the injured area of TBI rats. In addition, combining our results with the results from the above-mentioned published studies, we speculated that SCS might activate Akt phosphorylation to protect neurons.

In conclusion, we found that cSCS had a protective effect on neuron cells after craniocerebral injury and could improve neurological dysfunction in rats, the mechanism of which might be that cSCS made the PI3K/Akt pathway more active after TBI.

Acknowledgements

Conflicts of interest

There are no conflicts of interest.

References

1 Dewan MC, Rattani A, Gupta S, Baticulon RE, Hung YC, Punchak M, *et al.* Estimating the global incidence of traumatic brain injury [Epub ahead of print]. *J Neurosurg.* 2018:1–18.

2 Ng SY, Lee AYW. Traumatic brain injuries: pathophysiology and potential therapeutic targets. *Front Cell Neurosci* 2019;**13**:528.

3 Yamamoto S, Levin HS, Prough DS. Mild, moderate and severe: terminology implications for clinical and experimental traumatic brain injury. *Curr Opin Neurol* 2018;**31**:672–680.

4 Malinowski MN, Jain S, Jassal N, Deer T. Spinal cord stimulation for the treatment of neuropathic pain: expert opinion and 5-year outlook. *Expert Rev Med Devices* 2020;**17**:1293–1302.

5 Kuwahara K, Sasaki T, Yasuhara T, Kameda M, Okazaki Y, Hosomoto K, *et al.* Long-term continuous cervical spinal cord stimulation exerts neuroprotective effects in experimental Parkinson's disease. *Front Aging Neurosci* 2020;**12**:164.

6 Choi YH, Lee SU. Enhancement of brain plasticity and recovery of locomotive function after lumbar spinal cord stimulation in combination with gait training with partial weight support in rats with cerebral ischemia. *Brain Res* 2017;**1662**:31–38.

7 Xu Y, Li P, Zhang S, Wang Y, Zhao X, Wang X, Wang W. Cervical spinal cord stimulation for the vegetative state: a preliminary result of 12 cases. *Neuromodulation* 2019;**22**:347–354.

8 Gao YY, Zhang ZH, Zhuang Z, Lu Y, Wu LY, Ye ZN, *et al.* Recombinant milk fat globule-EGF factor-8 reduces apoptosis via integrin β3/FAK/PI3K/AKT signaling pathway in rats after traumatic brain injury. *Cell Death Dis* 2018;**9**:845.

9 Yuan B, Liu D, Liu X. Spinal cord stimulation exerts analgesia effects in chronic constriction injury rats via suppression of the TLR4/NF-κB pathway. *Neurosci Lett* 2014;**581**:63–68.

10 Sagher O, Huang DL, Keep RF. Spinal cord stimulation reducing infarct volume in a model of focal cerebral ischemia in rats. *J Neurosurg* 2003;**99**:131–137.

11 Zhang HB, Tu XK, Chen Q, Shi SS. Propofol reduces inflammatory brain injury after subarachnoid hemorrhage: involvement of PI3K/Akt pathway. *J Stroke Cerebrovasc Dis* 2019;**28**:104375.

12 Chen J, Li Y, Wang L, Zhang Z, Lu D, Lu M, Chopp M. Therapeutic benefit of intravenous administration of bone marrow stromal cells after cerebral ischemia in rats. *Stroke* 2001;**32**:1005–1011.

13 Greve MW, Zink BJ. Pathophysiology of traumatic brain injury. *Mt Sinai J Med* 2009;**76**:97–104.

14 Sulhan S, Lyon KA, Shapiro LA, Huang JH. Neuroinflammation and blood-brain barrier disruption following traumatic brain injury: Pathophysiology and potential therapeutic targets. *J Neurosci Res* 2020;**98**:19–28.

15 Malone C, Erler KS, Giacino JT, Hammond FM, Juengst SB, Locascio JJ, *et al.* Participation following inpatient rehabilitation for traumatic disorders of consciousness: a TBI Model systems study. *Front Neurol* 2019;**10**:1314.

16 Broseta J, García-March G, Sánchez-Ledesma MJ, Gonçalves J, Silva I, Barcia JA, *et al.* High-cervical spinal cord electrical stimulation in brain low perfusion syndromes: experimental basis and preliminary clinical report. *Stereotact Funct Neurosurg* 1994;**62**:171–178.

17 Sagher O, Huang DL. Effects of cervical spinal cord stimulation on cerebral blood flow in the rat. *J Neurosurg* 2000;**93**:71–76.

18 Wu M, Komori N, Qin C, Farber JP, Linderoth B, Foreman RD. Roles of peripheral terminals of transient receptor potential vanilloid-1 containing sensory fibers in spinal cord stimulation-induced peripheral vasodilation. *Brain Res* 2007;**1156**:80–92.

19 Wu M, Komori N, Qin C, Farber JP, Linderoth B, Foreman RD. Extracellular signal-regulated kinase (ERK) and protein kinase B (AKT) pathways involved in spinal cord stimulation (SCS)-induced vasodilation. *Brain Res* 2008;**1207**:73–83.

20 Li H, Dong X, Yang Y, Jin M, Cheng W. The neuroprotective mechanism of spinal cord stimulation in spinal cord ischemia/reperfusion injury. *Neuromodulation* 2021;**24**:43–48.

21 Deng H, Yue JK, Zusman BE, Nwachuku EL, Abou-Al-Shaar H, Upadhyayula PS, *et al.* B-Cell Lymphoma 2 (Bcl-2) and regulation of apoptosis after traumatic brain injury: a clinical perspective. *Medicina (Kaunas)* 2020;**56**:E300.

22 Bredesen DE. Programmed cell death mechanisms in neurological disease. *Curr Mol Med* 2008;**8**:173–186.

23 Yang L, Dong X, Zhang W. Astragaloside IV alleviates the brain damage induced by subarachnoid hemorrhage via PI3K/Akt signaling pathway. *Neurosci Lett* 2020;**735**:135227.

24 McCarthy KF, Connor TJ, McCrory C. Cerebrospinal fluid levels of vascular endothelial growth factor correlate with reported pain and are reduced by spinal cord stimulation in patients with failed back surgery syndrome. *Neuromodulation* 2013;**16**:519–22; discussion 522.

25 Uzan M, Erman H, Tanriverdi T, Sanus GZ, Kafadar A, Uzun H. Evaluation of apoptosis in cerebrospinal fluid of patients with severe head injury. *Acta Neurochir (Wien)* 2006;**148**:1157–64; discussion.

26 Lorente L, Martín MM, Argueso M, Ramos L, Solé-Violán J, Riaño-Ruiz M, *et al.* Serum caspase-3 levels and mortality are associated in patients with severe traumatic brain injury. *BMC Neurol* 2015;**15**:228.

27 Miñambres E, Ballesteros MA, Mayorga M, Marin MJ, Muñoz P, Figols J, López-Hoyos M. Cerebral apoptosis in severe traumatic brain injury patients: an *in vitro*, in vivo, and postmortem study. *J Neurotrauma* 2008;**25**:581–591.

28 Ahmed S, Kwatra M, Gawali B, Panda SR, Naidu VGM. Potential role of TrkB agonist in neuronal survival by promoting CREB/BDNF and PI3K/Akt signaling *in vitro* and *in vivo* model of 3-nitropropionic acid (3-NP)-induced neuronal death. *Apoptosis* 2021;**26**:52–70.

29 Saw G, Krishna K, Gupta N, Soong TW, Mallilankaraman K, Sajikumar S, Dheen ST. Epigenetic regulation of microglial phosphatidylinositol 3-kinase pathway involved in long-term potentiation and synaptic plasticity in rats. *Glia* 2020;**68**:656–669.

30 Tilley DM, Cedeño DL, Kelley CA, Benyamin R, Vallejo R. Spinal cord stimulation modulates gene expression in the spinal cord of an animal model of peripheral nerve injury. *Reg Anesth Pain Med* 2016;**41**:750–756.

31 Park JY, Shin MS. Inhibitory effects of pectic polysaccharide isolated from diospyros kaki leaves on tumor cell angiogenesis via VEGF and MMP-9 regulation. *Polymers (Basel)* 2020;**13**:E64.

32 Kilic E, Kilic U, Wang Y, Bassetti CL, Marti HH, Hermann DM. The phosphatidylinositol-3 kinase/Akt pathway mediates VEGF's neuroprotective activity and induces blood brain barrier permeability after focal cerebral ischemia. *FASEB J* 2006;**20**:1185–1187.

33 Shinko A, Agari T, Kameda M, Yasuhara T, Kondo A, Tayra JT, *et al.* Spinal cord stimulation exerts neuroprotective effects against experimental Parkinson's disease. *PLoS One* 2014;**9**:e101468.